Original

Child–Pugh Classification using Magnetic Resonance Imaging using Gadoxetic Acid–based Contrast Agent Compared with Indocyanine Green and ^{99m}Tc–galactosyl–human Serum Albumin Liver Scintigraphy

Enkhjargal Manduul[1,2], Takahito Nakajima[3], Kei Shibuya[4], Suman Shrestha[1], Hiromi Hirasawa[3], Yoshito Tsushima[1]

1 Department of Diagnostic Radiology and Nuclear Medicine, Gunma University Graduate School of Medicine, 3-39-22 Showa-machi, Maebashi, Gunma 371-8511, Japan
2 Department of Radiology, Mongolian National University of Medical Sciences, Ulaanbaatar, Mongolia
3 Department of Diagnostic Radiology, Interventional Radiology and Nuclear Medicine, Gunma University Hospital 3-39-15 Showa-machi, Maebashi, Gunma 371-8511, Japan
4 Gunma University Heavy Ion Medical Center, 3-39-22 Showa-machi, Maebashi, Gunma 371-8511, Japan

ABSTRACT

This study evaluated liver function using gadoxetic acid-enhanced magnetic resonance imaging (EOB-MRI) to improve assessment of patients with liver tumors compared to Child-Pugh classification (CPC). **Materials and methods:** The liver function of 59 patients was assessed to determine the indication for heavy ion therapy. Clinical and laboratory assessments, including ^{99m}Tc-GSA liver scintigraphy and indocyanine green retention index (ICGR15), were performed for liver function assessment. EOB-MRI was performed on T1W1 images both before and after Gd-EOB-DTPA administration and hepatobiliary phase images were acquired 20-min post-injection. Liver parenchymal enhancement ratio (LER) was measured based on liver-to-spleen (L/Sp) ratios calculating the average liver intensity divided by spleen intensity. **Results:** The mean LER values on MRI were 138.2 ± 12.8 (133.9－142.5), 115.7 ± 11.6 (110.0－121.5), and 93.2 ± 15.8 (73.6－112.9) in CPC-A, -B and -C, respectively. From the correlation between the LER on MRI and ICGR15 and parameters of ^{99m}Tc-GSA liver scintigraphy, LER on MRI was highly significantly correlated with ICGR15 ($r = -0.67$; $p < 0.0001$). **Discussion:** This study demonstrated that LER values on EOB-MRI could classify liver function and had high correlation with CPC and ICGR15.

Article Information

Key words:
Child-Pugh classification,
EOB,
MRI,
Liver function,
Hepatobiliary phase

Publication history:
Received: May 28, 2019
Revised: June 5, 2019
Accepted: June 6, 2019

Corresponding author:
Takahito Nakajima
Department of Diagnostic Radiology, Interventional Radiology and Nuclear Medicine, Gunma University Hospital 3-39-15 Showa-machi, Maebashi, Gunma 371-8511, Japan
Tel: +81−27−220−8401
E-mail: sojin@gunma-u.ac.jp

Introduction

The Child-Pugh classification (CPC) is widely used to estimate the liver function of patients with hepatic tumors before performing hepatic resection.[1-3] The extent of hepatic resection is determined based on CPC and estimated hepatic functional reserve.[4] CPC is calculated based on serum albumin level, serum total bilirubin level, prothrombin time ratio, presence of ascites, and hepatic encephalopathy. Patients are classified into three groups: CPC-A, -B and -C.[5] Before operation and other invasive therapies, the liver function and hepatic functional reserve should be carefully evaluated to prevent mortality and improve prognosis, thereby reducing the possibility of unexpected postoperative liver dysfunction.

Various assessment methods are currently used to estimate the liver function, including ^{99m}Tc-galactosyl-human serum albumin (^{99m}Tc-GSA) liver scintigraphy and indocyanine green retention rate at 15 min (ICGR15). Recently, several studies have evaluated liver function using gadoxetic acid-enhanced magnetic resonance imaging (EOB-MRI) to improve the assessment of patients with severe liver dysfunction.[6-11]

Gadoxetic acid (gadolinium ethoxybenzyl diethylenetriaminepentaacetic acid; Gd-EOB-DTPA; Primovist®; Bayer Schering Pharma AG, Berlin, Germany) is an MRI contrast agent specific to hepatocytes and is used to identify hepatic tumors. The organic anion transporter OATP1B, expressed on the hepatocyte membrane surface, plays a role in the uptake of Gd-EOB-DTPA. Liver MR images obtained using T1-weighted imaging (T1WI) are acquired before and after the intravenous administration of Gd-EOB-DTPA. The hepatobiliary phase of EOB-MRI reveals enhanced normal liver parenchymal tissue, and identifies various types of hepatic tumors because tumors, which are not normal hepatic tissue and generally do not express OATP1B3, are depicted as enhancement defects.

It has been generally accepted that the sufficient time to reach the hepatobiliary phase is 20 min after Gd-EOB-DTPA administration, which is a suitable delay to *detect liver lesions*.[6,12-14] However, obtaining sufficient liver enhancement to detect tumor lesions is difficult in patients with severe liver dysfunction due to the loss of or reduced function of hepatocytes.[15] Furthermore, whether 20 min after Gd-EOB-DTPA administration is the optimal delay to *assess liver function* remains unclear. Therefore, studies on EOB-MRI have been conducted[16-24] using various parameters and indices related to liver enhancement.

In this study, liver parenchymal enhancement ratio (LER) is used. LER is the ratio of liver intensity to spleen intensity (L/Sp ratio) in the hepatobiliary phase divided by L/Sp ratio without contrast enhancement. This study aimed to identify whether EOB-MRI correlated with CPC and compared EOB-MRI to other indices for hepatic functional reserve, such as ^{99m}Tc-GSA liver scintigraphy and ICGR15.

Materials and methods

Patients

This retrospective study was approved by the Institutional Review Board of Gunma University Hospital (approval number HS2016－085), and informed consent was waived. A total of 133 consecutive outpatients with hepatic tumors from the Gunma University Heavy Ion Medical Center (GHMC) were enrolled between September 2010 and March 2016. The liver function of all patients was assessed to determine the indication for heavy ion therapy. Clinical and laboratory assessments, including ^{99m}Tc-GSA liver scintigraphy and ICGR15, were performed for liver function assessment. EOB-MRI was performed to evaluate the extent and number of hepatic tumors. The inclusion criteria in this study were as follows: patients (a) who underwent EOB-MRI before and after Gd-EOB-DTPA administration using the same MR imaging parameters; (b) for whom the CPC was completed; (c) for whom the L/Sp ratio was calculated; and (d) in whom both ^{99m}Tc-GSA liver scintigraphy and ICGR15 were performed (Fig. 1).

Finally, 59 patients (41 males and 18 females; mean age, 74.4 ± 9.6 years) were included in this study: 56 with hepatocellular carcinoma and 3 with intrahepatic cholangiocarcinoma. Patient characteristics are summarized in Tables 1 and 2.

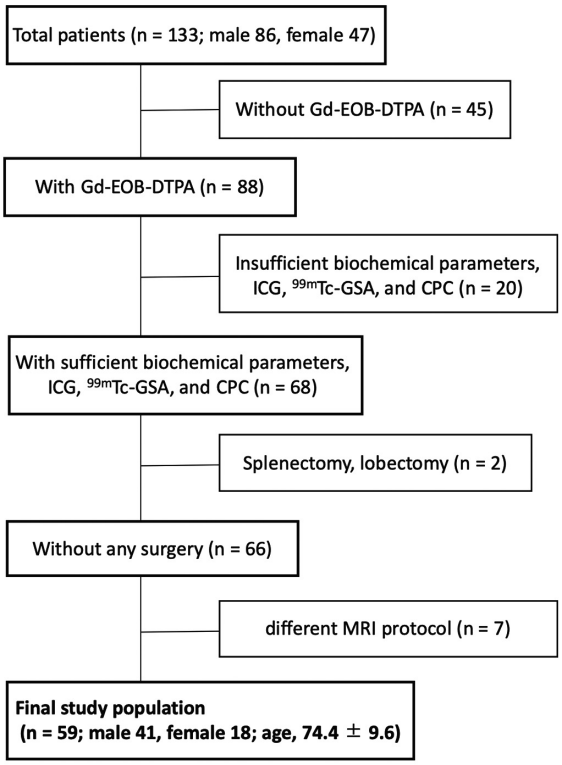

Fig. 1 Patient selection flowchart

Table 1 Patients' diagnoses and etiologies

	Child-Pugh classification		
	A	B	C
Disease			
HCC	33	18	5
ICC	3	0	0
Etiology			
Alcoholic	2	4	1
Hepatitis C	1	1	0
Hepatitis B with LC	6	3	0
Hepatitis C with LC	14	9	1
Both B and C virus	1	0	0
NASH/NAFLD	4	1	1
Normal liver	8	0	1
PBC	0	0	1

HCC, hepatocellular carcinoma; ICC, intrahepatic cholangiocarcinoma; PBC, primary biliary cirrhosis; LC, liver cirrhosis; NASH, nonalcoholic steatohepatitis; NAFLD, non-alcoholic fatty liver disease

99mTc-GSA liver scintigraphy

Before the injection of ^{99m}Tc-GSA, patients fasted for＞6 h. Liver scintigraphy was performed after an intravenous injection of 185 MBq of ^{99m}Tc-GSA (Nihon Medi-Physics, Nishinomiya, Japan). Regions of interest (ROIs) were placed on the liver and heart images. The liver uptake index (LHL15) was calculated as the

Table 2 Patient characteristics

Features	Child-Pugh classification			*p* value
	A	B	C	
Patients				
Age (years)	77.5 ± 7.4	72.3 ± 10.2	59.8 ± 6.1	＜0.0001*
Male/Female	29/7	9/9	3/2	0.064
Laboratory data				
WBC ($10^3\mu L^{-1}$)	4.8 ± 1.3	3.3 ± 0.9	5.9 ± 2.4	＜0.0001*
PT (%)	89.9 ± 18.1	80 ± 12.6	58.8 ± 35.2	0.002*
AST (U/L)	40.6 ± 31.6	51.2 ± 25.7	56.2 ± 24.5	0.317
ALT (U/L)	33.4 ± 29	31.0 ± 17.5	34.4 ± 13	0.934
LDH (U/L)	210.7 ± 63.7	211.1 ± 34.2	263 ± 133.8	0.233
ALP (U/L)	291 ± 168.2	345 ± 140.7	413.2 ± 153.3	0.197
γ GTP (U/L)	63.7 ± 72.7	70.2 ± 76.5	73.8 ± 58.6	0.928
ChE (U/mL)	251.4 ± 86.6	161.9 ± 46.4	118.4 ± 46.6	＜0.0001*
Plt ($/mm^3$)	163.5 ± 62.5	89 ± 47.9	151.6 ± 65.4	＜0.0001*
Alb (g/dL)	3.8 ± 0.3	3.3 ± 0.3	2.8 ± 0.4	＜0.0001*
Bil (mg/dL)	0.8 ± 0.2	1.2 ± 0.4	3.1 ± 2.2	＜0.0001*
NH_3 (μg/dL)	37.8 ± 23.5	75.6 ± 44	62.4 ± 58.8	0.001*

WBC, white blood cell; PT, prothrombin; AST, aspartate aminotransferase; ALT, alanine amino- transferase; LDH, lactate dehydrogenase; ALP, alkaline phosphatase; γGTP, gamma-glutamyl transferase; ChE, cholinesterase; Plt, platelets; Alb, albumin; Bil, bilirubin; NH_3, ammonia

* indicates statistical significance.

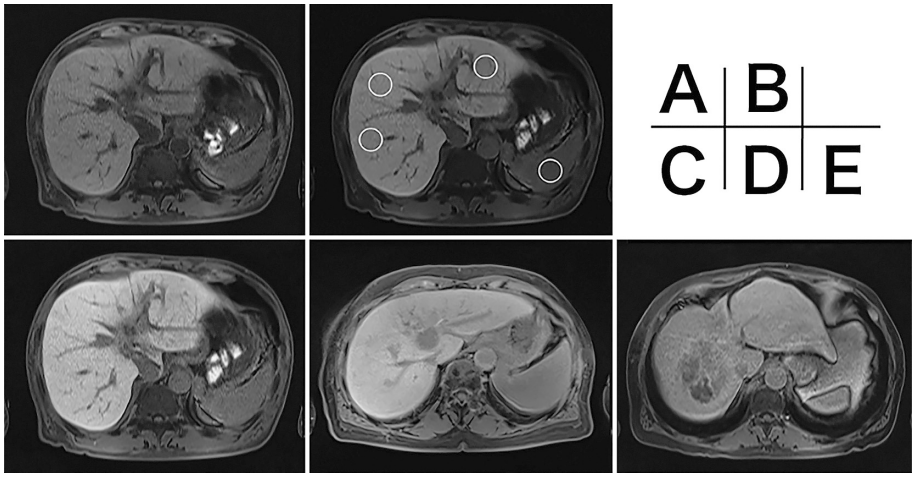

Fig. 2 Typical post-contrast EOB-MR images obtained in the hepatobiliary phase. Pre-contrast image in a patient with CPC-A (A). Regions of interest are drawn at three points in the liver and one point in the spleen (B). Representative images obtained on the hepatobiliary phase of patients with CPC-A (C), -B (D), and -C (E).

ratio between the liver count and the liver plus heart counts on the anterior view obtained from the static image 15 min after ^{99m}Tc-GSA injection. The clearance ratio (HH15) was calculated as the ratio of the heart counts at 3 and 15 min after the injection.

Clearance test of ICG (ICGR15)

After collecting the basal blood samples, ICG was administered via the arm vein at a dose of 0.5 mg/kg. A blood sample was collected from the opposite arm 15 min after the injection. ICGR15 was calculated as the blood clearance of ICG at 15 min.

EOB-MRI acquisition

MRI was performed using a 3.0T MR system (Skyra; Siemens Healthcare, Erlangen, Germany) and an 8-channel body-phased array coil. A standard single injection of Gd-EOB-DTPA was administered at a dose of 0.1 mL/kg body weight, followed by a 20 mL saline flush injected at a rate of 3 mL/s. T1WI images with fat saturation were obtained before and after Gd-EOB-DTPA administration, and hepatobiliary phase images were acquired 20 min after the injection. T1-weighted volumetric interpolated breath-hold examination (VIBE) was performed to obtain T1WI images. The imaging parameters of the VIBE sequence were as follows: TR/TE, 3.41/1.26 ms; flip angle, 10°; matrix, 320 × 168; slice thickness, 3 mm; and slice number, 60.

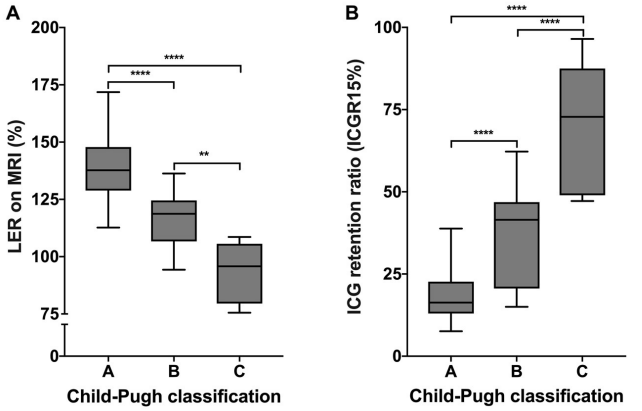

Fig. 3 (A) The LER values obtained on MRI and Child-Pugh classification (CPC). The LER values obtained on MRI values shows significant differences among the CPC groups (A and B or C, $p<0.0001$; B and C, $p<0.01$). (B) The ICG retention ratio and CPC. A significant difference is observed among the CPC groups ($p<0.0001$).

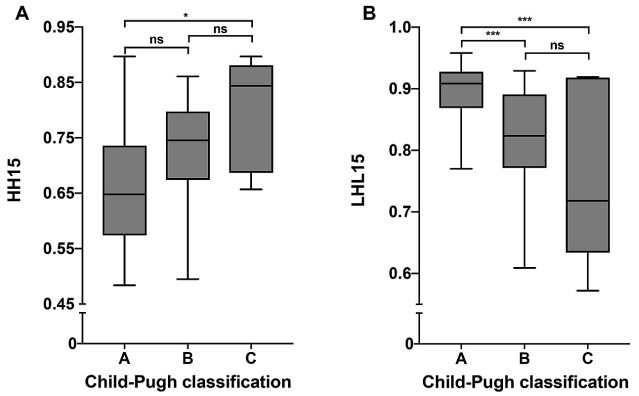

Fig. 4 The box plot represents the ^{99m}Tc-GSA values in Child-Pugh classification (CPC). (A) The HH15 was significantly different between the CPC-A and -C ($p=0.02$). (B) Comparisons of ^{99m}Tc-GSA values between CPC-A and -B or -C scores show a significant difference in terms of LHL15 among the CPC groups ($p<0.001$).

Liver parenchymal enhancement ratio (LER) on MRI

Three ROIs and one ROI were placed on the liver (the anteroposterior and lateral segments), and the spleen images on a representative slice of both the pre-contrast and the hepatobiliary phase MR images, respectively. The round-shaped ROIs measured 2 cm in diameter, and the average liver intensities in the ROIs were calculated. The L/Sp ratio was calculated using the following formula: average liver intensity/spleen intensity. Then, the LER was defined as the ratio of the L/Sp ratio in the hepatobiliary phase to that without contrast enhancement (Fig. 2).

Statistical analysis

All statistical analyses were performed using the GraphPad 7.0 software for Windows (GraphPad, California, USA) and SPSS 24.0 for Windows (IBM, New York, USA). Laboratory data of the CPC groups were analyzed using one-way analyses of variance (ANOVAs). Statistical differences in terms of the liver function indices at each clinical stage of the CPC were tested using ANOVAs and multiple comparisons with Bonferroni correction. Pearson's correlation coefficients were computed to assess the correlation between MRI-based liver function indices and biochemical parameters. ROC analyses were performed to examine the sensitivity, specificity, positive predictive value, negative predictive value, and accuracy of each liver function parameter. Then, area under the curve (AUC) was calculated using the ROC curve. All data are expressed as mean ± standard deviation (SD) and p-values of <0.05 were considered to indicate statistical significance.

Results

Patient characteristics

A total of 59 patients (41 males and 18 females) were included in this study: 36, 18, and 5 of them were classified into CPC-A, -B, and -C, respectively. The CPC and etiologies of chronic liver diseases are shown in Table 1.

Relationship between the Child–Pugh classification and biochemical parameters

Table 2 shows various parameters of clinical laboratory data in each CPC group. Prothrombin time (PT) and choline esterase (ChE), platelet (Plt), albumin (Alb), bilirubin (Bil), and ammonia (NH_3) levels showed significant differences among the CPC groups. PT and ChE, Alb, and Bil levels were dependent of the CPC. The patients in CPC-B had the highest Plt levels among the three groups.

Comparison of the LER values obtained on MRI and other liver function parameters among the CPC groups

The mean LER values obtained on MRI were 138.2 ± 12.8 (95% confidence interval [CI], 133.9 − 142.5), 115.7 ± 11.6 (110.0 − 121.5), and 93.2 ± 15.8 (73.6 − 112.9) for the CPC-A, -B and -C, respectively. The ANOVA ($F=10.9$, $p<0.0001$) and post-hoc multiple comparisons with Bonferroni correction showed significant differences among all CPC groups in this regard (Fig. 3A).

The ICGR15 test mean values were 18.3 ± 7.8 (15.7 − 20.9), 35.9 ± 14.8 (28.6 − 43.3), and 69.1 ± 20.4 (43.8 − 94.5) for CPC-A, -B, and -C groups, respectively. ANOVA ($F=31.5$, $p<0.0001$) demonstrated that the ICGR15 test showed significant differences among the CPC groups (A to B, $p<0.0001$; B to C, $p<0.0001$; and C to A, $p<0.0001$, Fig. 3B).

ANOVA ($F=7.31$, $p=0.0015$) followed by post-hoc comparisons with Bonferroni correction indicated that only clearance indices (HH15) of ^{99m}Tc-GSA liver scintigraphy were significantly different between the CPC-A and -C [0.659 ± 0.108 (0.631 − 0.687) vs. 0.796 ± 0.103 (0.667 − 0.924); $p<0.05$]. Meanwhile, an ANOVA (F=

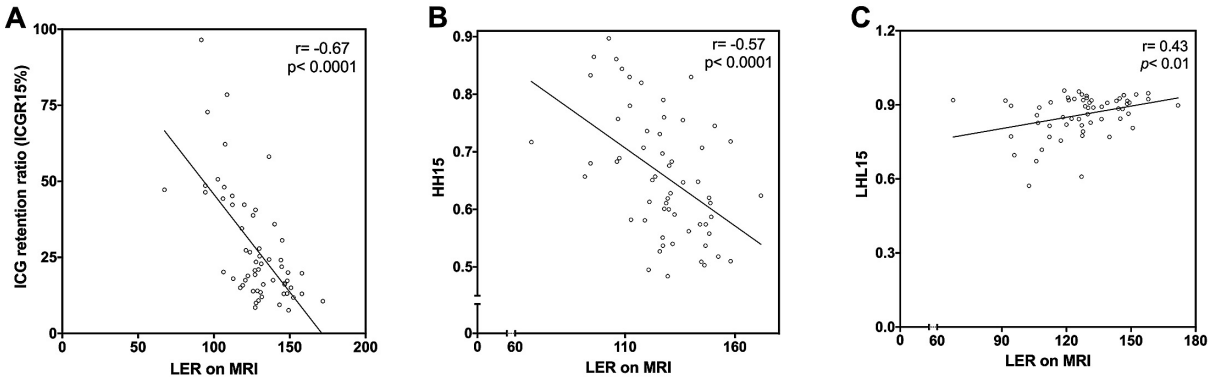

Fig. 5 Correlation between the LER values obtained on MRI and ICG retention (A), HH15 (B), and LHL15 (C). The LER values obtained on MRI is moderately correlated with ICG retention (r＝－0.67; $p<0.0001$), HH15 (r＝－0.57; $p<0.0001$), and LHL15 (r＝0.43; $p<0.01$).

5.852; $p=0.0048$) showed that LHL15 significantly differed between the CPC-A and -B [0.896 ± 0.044 (0.880－0.911) vs. 0.817 ± 0.085 (0.774－0.859); $p<0.001$] and CPC-A and -C [0.896 ± 0.04 (0.77－0.96) vs. 0.764 ± 0.150 (0.577－0.951); $p<0.001$]. However, no statistically significant difference was observed in terms of LHL15 between the CPC-B and -C (Fig. 4).

Correlation between the LER values obtained on MRI and ICGR15 and 99mTc-GSA parameters

Fig. 5 shows the correlations between the LER values obtained on MRI and liver function parameters. The correlation coefficients (r) of the LER values obtained on MRI, HH15 and LHL were r＝－0.57 ($p<0.0001$) and r＝0.43 ($p<0.01$), respectively. The LER values obtained on MRI were highly significantly correlated with ICGR15 (r＝－0.67; $p<0.0001$).

ROC curve analyses of various parameters

The performance evaluation of each parameter to differentiate among the CPC groups and the optimal cut-off levels are described in Table 3. The use of LER values obtained on the MRI cut-off level of 127.1 to dif-

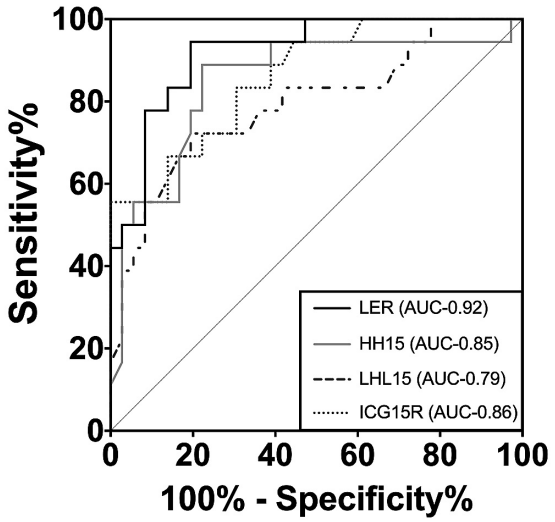

Fig. 6 Receiver operating characteristic (ROC) curves for LHL15, HH15, the LER values obtained on MRI ratio, and ICG retention to differentiate the CPC groups.

Table 3 ROC curve analysis among liver functional indices to classify CPC

Child-Pugh	Parameters	Cut-off	AUC	Sensitivity	Specificity	*p* value
A and B	LER on MRI	＜127.1	0.92	83.3	86.1	＜0.0001*
	HH15	＞0.649	0.85	88.9	77.8	＜0.0001*
	LHL15	＜0.86	0.79	72.2	80.6	0.0005*
	ICG15R	＞23.2	0.86	72.2	77.8	＜0.0001*
B and C	LER on MRI	＞106.2	0.89	83.3	80.3	0.0091*
	HH15	＜0.84	0.72	94.4	60.2	ns
	LHL15	＞73.6	0.62	88.9	60.1	ns
	ICG15R	＜46.8	0.93	77.8	100	0.003*
C and A	LER on MRI	＜110.7	1	100	100	0.0003*
	HH15	＞0.712	0.93	80	88.9	0.0019*
	LHL15	＜0.74	0.74	60	100	0.0904
	ICG15R	＞43	1	100	100	0.0003*

AUC, area under the curve; LER on MRI, Liver enhancement ratio on MRI; HH15, an index of blood clearance; LHL15, a receptor index; ICG15R, indocyanine green retention rate at 15 min

* indicates statistical significance.

ferentiate between CPC-A and -B was associated with a sensitivity of 83.3% and specificity of 86.1% (AUC, 0.92). A threshold level of 0.649 for HH15 was associated with a sensitivity of 88.9% and specificity of 77.8% (AUC, 0.85). Similarly, a threshold level of 0.86 for LHL15 to distinguish between CPC-A and -B was associated with a sensitivity of 72.2% and specificity of 80.6% (AUC, 0.79). The optimal cut-off level for ICG15R was associated with a sensitivity of 72.2% and specificity of 77.8% (AUC, 0.86; Fig. 6 and Table 3).

Discussion

This study demonstrated that the LER values obtained on EOB-MRI could classify liver function, correlating with the CPC. Several studies on EOB-MRI have evaluated the methods used for the estimation of image-based liver functional estimation and reserve. The relative enhancement (RE) ratios of the liver on EOB-MRI represent an increased ratio of signal intensities of the liver after the Gd-EOB-DTPA administration as compared with the initial values. Kubota et al. investigated the correlations between maximal RE values and liver damage scores in 41 patients with suspected hepatocellular carcinoma (HCC).[7] The maximal RE values were shown to be correlated with the patients' laboratory data in the univariate analyses, reflecting the liver function and ICGR15. Tamada et al. reported an RE investigation in the hepatobiliary phase using EOB-MRI at three time points (10, 15, and 20 min).[25] The mean RE of the liver parenchyma significantly increased at 20 min after the injection in patients with CPC-A, whereas no increasing tendency of RE was observed in patients with CPC-C. The mean RE of the liver parenchyma was the highest in the normal liver, followed by in CPC-A, -B and -C. Therefore, hepatic parenchymal enhancement on EOB-MRI reflecting RE was affected by the severity of cirrhosis.

Motosugi et al. introduced the liver-spleen contrast to calculate the LER and examined whether the examination time required to acquire the hepatobiliary phase image can be shortened. They assessed the RE value for the hepatobiliary phase images at 10 and 20 min after Gd-EOB-DTPA administration using the visual liver-spleen contrast scale (V-LSC) and quantitative liver-spleen contrast ratio (Q-LSC). They concluded that the liver-spleen contrast was sufficient 10 min after Gd-EOB-DTPA administration.[8]

This study focused on the correlation between the LER values obtained on EOB-MRI and CPC. LERs on EOB-MRI were calculated using the liver-spleen contrast at 20 min after injection. The ROC analyses used to evaluate the classification ability of each liver function parameter between CPC-A and -B, CPC-B and -C, and CPC-C and -A revealed that the LER values obtained on EOB-MRI and ICGR15 showed a moderate-to-high correlation with CPC. The LER and ICGR15 yielded high AUC values in each ROC analysis. The ^{99m}Tc-GSA liver scintigraphy could differentiate CPC-A and -C, but not CPC-B and -C or CPC-C and -A.

Comparison between the LER values obtained on EOB-MRI and ICGR15 revealed a good negative linear correlation ($r=-0.67$), whereas that between the LER values obtained on EOB-MRI and ^{99m}Tc-GSA liver scintigraphy index, HH15, was weak ($r=-0.57$). Our results indicate that the LER values obtained on EOB-MRI and ICGR15 would similarly work as the functional indices for the estimation of liver function or hepatic functional reserve. Conversely, ^{99m}Tc-GSA liver scintigraphy might be an independent factor for the assessment of liver function. Some patients who were CPC-A showed poor prognosis after hepatic resection, and the effort to find good prognostic factors are underway. Therefore, this study showed that ^{99m}Tc-GSA liver scintigraphy was independent of LER on EOB-MRI and ICGR15 in estimating liver function.

Recently, Yoneyama et al. investigated the liver function index that combined liver enhancement and liver volume. They proposed the use of functional liver volume, calculated by multiplying the LER or RE by the liver volume. Studies such as that by Yoneyama et al. have introduced the use of functional liver volume in addition to the LER or RE, which yield similar results.[19] However, the extent of additional improvement for the assessment of liver function was not necessarily exceptional compared with that observed for other studies. In addition, using a complicated formula with multiplied parameters would emphasize the variabilities of liver function values from MRI studies.

These results suggest that the focal liver function of normal livers would be better than the liver function level estimated from focal liver volumes, or that focal liver function would be alternatively increased to compensate the liver damage or resected areas. Because EOB-MRI has a high spatial resolution, it would have the potential to reflect local function of the liver parenchyma.

Sourbron et al. investigated the combined quantification of liver perfusion and function using EOB-MRI and provided Khep liver images. Khep theoretically reflects the actual function of hepatocytes related to Gd-EOB-DTPA uptake and could be used to assess regional hepatic functional reserves in the future. In clinical studies, liver images obtained in the hepatobiliary phase were acquired 20 min after Gd-EOB-DTPA administration, which is also used to detect hepatic tumors.[20] However, to evaluate liver function, an earlier acquisition such as at 10 min, as in the liver data provided by Motosugi, might provide more useful information reflecting the actual function of hepatocytes.[8]

The limitation of this study is the small number of patients classified into CPC-C. Because a candidate for heavy ion therapy would have a relatively healthy liver and a small number of hepatic tumors, the sample size of patients in CPC-A and -B in this study was sufficiently large. However, in the future, if regional liver function can be evaluated, heavy ion beam therapy plans can take advantage of the focally impaired area to reduce the effects on total liver function.

In conclusion, this study demonstrated that CPC, EOB-MRI, and ICGR15 are highly correlated to one another and also with CPC, and that ^{99m}Tc-GSA liver scintigraphy was a factor independent of EOB-MRI. The results also suggest that liver function assessment should be performed prior to administering treatment using both ^{99m}Tc-GSA liver scintigraphy and EOB-MRI to promote safe patient management.

References

1. Schneider PD. Preoperative assessment of liver function. Surg. Clin. North Am 2004; 84: 355-373.
2. Kaplan DE, Dai F, Aytaman A, et al. Development and performance of an algorithm to estimate the child-turcotte-pugh score from a national electronic healthcare database. Clin Gastroenterol Hepatol 2015; 13: 2333-2341.e6.
3. Durand F, Valla D. Assessment of prognosis of cirrhosis. Semin Liver Dis 2008; 28: 110-122.
4. Garcea G, Ong SL, Maddern GJ. Predicting liver failure following major hepatectomy. Dig Liver Dis 2009; 41: 798-806.
5. Pugh RNH, Murray-Lyon IM, Dawson JL, et al. Transection of the oesophagus for bleeding oesophageal varices. Br J Surg 1973; 60: 646-649.
6. Sourbron S, Sommer W, Reiser M, et al. Combined quantification of liver perfusion and function with dynamic gadoxetic acid-enhanced MR imaging. Radiology 2012; 263: 874-883.
7. Kubota K, Tamura T, Aoyama N, et al. Correlation of liver parenchymal gadolinium-ethoxybenzyl diethylenetriamine-pentaacetic acid enhancement and liver function in humans with hepatocellular carcinoma. Oncol Lett 2012; 3: 990-994.
8. Motosugi U, Ichikawa T, Tominaga L, et al. Delay before the hepatocyte phase of Gd-EOB-DTPA-enhanced MR imaging: Is it possible to shorten the examination time? Eur Radiol 2009; 19: 2623-2629.
9. Leinhard OD, Dahlstrom N, Kihlberg J, et al. Quantifying differences in hepatic uptake of the liver specific contrast agents Gd-EOB-DTPA and Gd-BOPTA: A pilot study. Eur Radiol 2012; 22: 642-653.
10. Nishie A, Ushijima Y, Tajima T, et al. Quantitative analysis of liver function using superparamagnetic iron oxide- and Gd-EOB-DTPA-enhanced MRI: Comparison with technetium-99m galactosyl serum albumin scintigraphy. Eur J Radiol 2012; 81: 1100-1104.
11. Yamada A, Hara T, Li F, et al. Quantitative evaluation of liver function with use of gadoxetate disodium-enhanced MR imaging. Radiology 2011; 260: 727-733.
12. Vogl TJ, Kümmel S, Hammerstingl R, et al. Liver tumors: Comparison of MR imaging with Gd-EOB-DTPA and Gd-DTPA. Radiology 1996; 200: 59-67.
13. Hamm B, Staks T, Mühler A, et al. Phase I clinical evaluation of Gd-EOB-DTPA as a hepatobiliary MR contrast agent: safety, pharmacokinetics, and MR imaging. Radiology 1995; 195: 785-792.
14. Saito K, Ledsam J, Sourbron S, et al. Assessing liver function using dynamic Gd-EOB-DTPA-enhanced MRI with a standard 5-phase imaging protocol. J Magn Reson Imaging 2013; 37: 1109-1114.
15. Narita M, Hatano E, Arizono S, et al. Expression of OATP1B3 determines uptake of Gd-EOB-DTPA in hepatocellular carcinoma. J Gastroenterol 2009; 44: 793-798.
16. Utsunomiya T, Shimada M, Hanaoka J, et al. Possible utility of MRI using Gd-EOB-DTPA for estimating liver functional reserve. J Gastroenterol 2012; 47: 470-476.
17. Okada M, Murakami T, Kuwatsuru R, et al. Biochemical and clinical predictive approach and time point analysis of hepatobiliary phase liver enhancement on Gd-EOB-DTPA enhanced MR images: A multicenter study. Radiology 2016; 281: 474-483.
18. Nilsson H, Nordell A, Vargas R, et al. Assessment of hepatic extraction fraction and input relative blood flow using dynamic hepatocyte-specific contrast-enhanced MRI. J Magn Reson Imaging 2009; 29: 1323-1331.
19. Yoneyama T, Fukukura Y, Kamimura K, et al. Efficacy of liver parenchymal enhancement and liver volume to standard liver volume ratio on Gd-EOB-DTPA-enhanced MRI for estimation of liver function. Eur Radiol 2014; 24: 857-865.
20. Saito K, Kotake F, Ito N, et al. Gd-EOB-DTPA enhanced MRI for hepatocellular carcinoma: Quantitative evaluation of tumor enhancement in hepatobiliary phase. Magn Reson Med Sci 2005; 4: 1-9.
21. Haimerl M, Verloh N, Zeman F, et al. Gd-EOB-DTPA-enhanced MRI for evaluation of liver function: Comparison between signal-intensity-based indices and T1 relaxometry. Sci Rep 2017; 7: 43347.
22. Motosugi U, Ichikawa T, et al. Liver parenchymal enhancement of hepatocyte-phase images in Gd-EOB-DTPA-enhanced MR imaging: Which biological markers of the liver function affect the enhancement? J Magn Reson Imaging 2009; 30: 1042-1046.
23. Yamada S, Shimada M, Morine Y, et al. A new formula to calculate the resection limit in hepatectomy based on Gd-EOB-DTPA-enhanced magnetic resonance imaging. PLoS One 2019; 14: e0210579.
24. Motosugi U, Ichikawa T, Oguri M, et al. Staging liver fibrosis by using liver-enhancement ratio of gadoxetic acid-enhanced MR imaging: Comparison with aspartate aminotransferase-to-platelet ratio index. Magn Reson Imaging 2011; 29: 1047-1052.
25. Tamada T, Ito K, Higaki A, et al. Gd-EOB-DTPA-enhanced MR imaging: Evaluation of hepatic enhancement effects in normal and cirrhotic livers. Eur J Radiol 2011; 80: e311-e316.